Wurtzite AlP_yN_{1-y}: A New III-V Compound Semiconductor Lattice Matched to GaN (0001)

Markus Pristovsek,[1*] Duc van Dinh,[1†], Ting Liu,[1,2] and Nobuyuki Ikarashi[1]

[1] *Center for Integrated Research of Future Electronics, Institute for Materials and Systems for Sustainability, Nagoya University, 1 Furo-cho, Chikusa-Ku, Nagoya, 464-8603, Japan*

[2] *National Institute for Materials Science, 1 Chome-1 Namiki, Tsukuba 305-0044, Japan*

We report on a new member of III-Nitride family, wurtzite AlP_yN_{1-y}, tensile strained or lattice matching (at $\approx 10.6\,\%$ P) on (0001) GaN. Unlike lattice matched AlInN, AlP_yN_{1-y} can be grown between 1050°C to 1250°C under hydrogen atmosphere in metal-organic vapor phase epitaxy. The transition from GaN to AlP_yN_{1-y} is sharp, there is no Ga carry over. Due to the small P content, physical properties like bandgap (around 5.5 eV), dielectric function, or polarisation are close to AlN. A first unoptimized AlPN/GaN heterostructure shows a low sheet resistance of $150 \pm 50\,\Omega/\square$, which makes AlP_yN_{1-y} promising for electronic applications.

Despite many contenders, GaN based semiconductors are still by far the most important semiconductors after silicon. Commercial devices use hetero-structures of ternary alloys of $Al_xGa_{1-x}N$ or $In_xGa_{1-x}N$ and are grown with metal-organic vapor phase epitaxy (MOVPE). However, AlGaN is tensilely and InGaN compressively strained to GaN, which limits many applications. The compound $Al_{0.83}In_{0.17}N$ is lattice matched to GaN. AlInN has been used for Bragg mirrors [1] but the low growth rate and temperature ramping makes it unsuitable for industrial use. AlInN is also researched for base layer in high electron mobility transistors (HEMTs), but a strong challenge is the initial incorporation of Ga into the AlInN layers [2–4].

Recently $Al_{1-x}Sc_xN$ has been grown on GaN by MOVPE [5, 6] as base layer in HEMTs. However, the precursor tris-cyclopentadienyl scandium has a very low vapor pressure which requires heavy modifications of the MOVPE system (gas mixing system and showerhead at 150°C), and the precursor has 15 carbon atoms per Sc atom.

Thus, a lattice matched alloy is desired that is easy to grow on GaN, with properties close to AlN, and has a suitable precursor. We demonstrate that AlP_yN_{1-y} can be

*E-mail: pristovsek@imass.nagoya-u.ac.jp

†present address: Paul Drude Institute Berlin, Germany

lattice matched to GaN, grown at similar growth conditions as GaN, and even has some superior physical properties compared to AlInN.

Alloying of P into AlGaN using MOVPE has been first proposed in an already expired patent [7], which claimed $Al_xGa_{1-x}P_yN_{1-y}$ with $y < 0.0025$ for strain reduction in AlGaN cladding layers in laser diodes. However, there has been no associated publication. Thus, it is unclear if these layers have been ever made in practice. In comparison, alloying of P into wurtzite GaN had been studied by a few groups around the turn of the century e.g. [8–16]. From these reports one can extract a bandgap bowing of about 9 eV using 2.1 eV for the bandgap of wurtzite GaP [17]. Even though a light emitting diode (LED) was realized [13] the efforts came to a halt, because GaP_yN_{1-y} exhibits P-related defect formation for $y > 3\,\%$ [9–11, 16]. Even visible in optical microscopy were cubic or P-rich domains. But most important, P atoms started to incorporate on the Ga lattice site or even formed P_3N_3 domains. Since GaP_yN_{1-y} is compressively strained on GaN, GaPN can reduce its strain energy by P replacing Ga atoms (and losing stoichiometry), because the bond length of P_3N_3 is shorter than in GaP or GaN [16]. This could occur in AlP_yN_{1-y} too, since the covalent radii of P (107 pm) is larger than that of N (71 pm), but not so much smaller than Al (121 pm) or Ga (122 pm). Thus, tensile strained or lattice matched AlP_yN_{1-y} alloys should keep the P on the group V lattice sites. This motivated the current work.

There are two mature precursors for growth of P-containing compounds like InGaP or AlGaInAsP. Cheap and carbon free is PH_3 gas. But its use is forbidden due to its toxicity in many laboratories including ours. The alternative is the liquid metal-organic precursor tertiary-butylphosphine (tBP), which has a relatively high vapor pressure, is less toxic, and decomposes at even lower temperatures than PH_3 [18].

The AlP_yN_{1-y} layers were grown on (0001) GaN on sapphire templates using a closed coupled 3×2" MOVPE reactor from EpiQuest. The carrier gas was hydrogen between 5-20 kPa reactor pressure, with trimethyl aluminum (TMAl), NH_3, and tBP. For the tBP vapor pressure we used $p_{tBP}(Torr) = 10^{7.552-1529/T(K)}$ from the data sheets of Dockweiler.

The growth of group V-interface usually requires special attention to avoid heteroexchange. To initiate AlPN growth, first we switched on TMAl and tBP on together. For later samples, tBP flow was switched on a few seconds before TMAl. After growth the AlPN layers were cooled to 950°C with tBP and NH_3 flowing, and were switched off during further cooling.

Currently, tBP is injected via an empty MO line. This is not ideal, because gas phase reactions have been reported for the growth of AlGaP using tBP [19]. Moreover, the tBP partial pressure of up to 22 Pa exceeds the TMAl vapor pressure of $\leq$0.35 Pa by far, so there is a good chance of pre-reactions inside the lines and the showerhead. For this reasons all reactors usually separate lines for group III and group V precursors, and moving tBP to group V inlet is planned.

The XRD measurements were performed using different four axis diffractometers. The simulated spectra are based on a software originally published for semipolar layers [20]. The lattice constants of wurtzite AlP were calculated by the materials project [21] and then corrected by the same factor than was needed to match the calculated to the experimental determined lattice constant of wurtzite GaP [17]. The elastic tensor elements of wurtzite AlP were directly taken from the materials project [21].

Spectroscopic ellipsometry was measured using a Jobin Yvon photo-elastic modulator variable angle ellipsometer between 1.5 and 6.5 eV. The data were then numerically fitted with a five layer stack (sapphire, GaN, AlPN, AlPN 1-8 nm 50 % Bruggeman roughness layer, and air). To ensures a Kramer-Kronig consistency over the whole spectral range, an ϵ_2 spline was Kramer-Kronig transformed as AlPN dielectric function for fitting [22]. Additionally, the refractive index n was extracted in the transparent region from the extrema in vertical incidence reflection measurements, similar to the Swanepoel method in transmission [23].

Transmission electron microscopy (TEM) was measured in a JEOL ARM 200F instrument, which was used in high angle annular dark field scanning TEM as well as in bright field TEM configuration. The instrument was also equipped with energy dispersive X-ray spectroscopy (EDS).

In the initial series of experiments, thin AlPN layers (20-45 nm) were grown with increased tBP partial pressure while all other parameters were kept constant. With increasing tBP partial pressure the number of cracks drastically reduced (inset in figure 1).

In order to explore the incorporation limits of strained AlP_yN_{1-y}, next a series of AlP_yN_{1-y}/GaN superlattices were grown with nominal thicknesses of 7 nm AlPN/14 nm GaN. As it can be seen from figure 1 the satellite peaks in X-ray diffraction (XRD) vanish for condition which would result in an extrapolated P-content of 18-20 %, i.e. for compressive strain. However, the satellite peaks remain visible for high tensile strain up to AlN. Therefore, compressive strain is detrimental to AlP_yN_{1-y}, as it was expected

from the reports for GaP_yN_{1-y}. However, the P incorporation has a delay, which is discussed later, and which probably explain the rather wide satellite peaks which obscure the fringe oscillations.

Thicker layers using the lattice matched growth conditions from the superlattices were visibly dark (see supplemental). Since AlN at similar growth conditions remains transparent, the main suspect is carbon from the P precursor tBP. This is at first unexpected, since tBP decomposes at lower temperatures than PH_3 [18] and thus InGaP incorporates less carbon using tBP. However, at temperatures exceeding 800°C-900°C all linear carbohydrate chains C_xH_y decompose into single CH_x radicals [24]. For the same reason triethyl Ga incorporates more carbon at high temperatures than trimethyl Ga [25]. Thus, at 1050°C or higher the total number of carbon atoms counts. The tBP partial pressure is about 50× higher than the TMAl partial pressure, and tBP contains 4 carbon atoms instead 3 for TMAl. Hence, during AlPN growth about 70× more CH_x radicals are present than for AlN growth. Since carbon free PH_3 is forbidden in our laboratory, we increased the NH_3 partial pressure to supply more active hydrogen to the surface. Interestingly, the higher NH_3 flow did not reduce the P incorporation much, but it made a several 100 nm thick AlPN layer almost transparent.

Figure 2 show a wide area XRD $\omega - 2\Theta$ measurement of a lattice matched AlPN layer, including a tBP-preflow and after growth stabilisation. There are only reflections related to GaN, sapphire and $AlP_{10.3}N_{89.7}$. No signals were found of any of the allowed cubic AlP reflections (dotted lines in figure 2). Hence the layer is pure wurtzite AlPN. The bottom half shows the (0002) reflection together with simulated data. According to the quantitative XRD simulation, the layer in figure 2 has 10.3 % P content. Perfect lattice matching would be at 10.6% P, thus it is slightly tensilely strained. The XRD reciprocal space map of the $(10\bar{1}5)$ reflection (inset in figure 2) confirms that the AlPN is fully strained.

We extracted the dielectric function from ellipsometry measurements of three samples with thicknesses from 120 nm to 655 nm. The resulting Kramers Kronig consistent dielectric function is shown in figure 3. However, the phase modulated ellipsometer has less accuracy in the transparent region. The position of maxima and minima in vertical incidence reflectance measurements can give higher accuracy in the transparent region, because the only parameter is the thickness of the layer which was determined from cross section SEM measurements. Both analysis support a refractive index around 1.95-2.05 in the transparent region, close to the value reported for AlN (cf. [26]). Com-

pared to $Al_{0.83}In_{0.17}N$ [1] the refractive index difference of $AlP_{0.11}N_{0.89}$ to GaN is about 2× larger. Hence, a Bragg mirror from $AlP_{0.11}N_{0.89}$ could reach 99 % reflectivity with only 14 pairs for wavelengths between 300 and 550 nm. Because the AlPN growth rate was around 700 nm/h for our samples, and no temperature ramping or gas exchanges are needed, an entire Bragg mirror would take less than 2-3 hours growth time. This compares favourably with the 12 hours or more of growth time typical for AlInN Bragg mirrors, which is mostly limited by temperature ramping between AlInN and GaN layers. (Unfortunately with the current tBP injection via group III inlet, too much tBP-TMAl adduct accumulated in the lines and on the showerhead, which led to a P-gradient in the structure and subsequent cracking.)

The inset in figure 3 shows that Fabry Pérot (FP) oscillations of 655 nm thick $AlP_{0.13}N_{0.87}$ layer were visible up to about 5.5 eV. This points to a bandgap around 5.5 eV. Assuming a similar bandgap bowing as wurtzite GaP_yN_{1-y} (9 eV) and a direct bandgap of 3.4 eV for wurtzite AlP, at 13 % P one would expect a bandgap of 5 eV for $AlP_{0.13}N_{0.87}$. However, the band bowing of GaP_yN_{1-y} has a large error. Assuming instead a 5.5 eV bandgap at 13 % would result in a moderate bandgap bowing of 3 eV for AlP_yN_{1-y}. Since cathodoluminescence was inconclusive (see supplemental), the bandgap is still under investigation.

Since the P-content is low, a very high polarisation is expected, close to AlN. This would induce high carrier concentrations in HEMT structure. Indeed, a sheet resistance mapping gave a low value of $(150 \pm 50)\Omega/\square$, even though the sample was not optimised. A mean value of 150 $\Omega/\square$ would be an excellent values for a AlInN/AlN/GaN heterostructure (e.g. [27]), and at least on the same order as the $Al_{1-x}Sc_xN$ system [6], which is expected to have a high polarisation too.

One inherent challenge must be mentioned. Pure cubic AlP tend to oxidize quickly, its reacts with the ambient moisture to Al_2O_3 within seconds after being removed from the MOVPE reactor, while releasing PH_3. The fast oxidation has been even used to form Al_2O_3 passivation layers quasi in-situ from AlP [28] upon removal from the reactor. Also cubic fcc AlAs oxidizes fast, which is used to define current apertures in vertical cavity lasers or single quantum dots devices. However, alloying with Ga strongly reduce this oxidation rate, and similar can be expected for AlPN. AlPN is not as unstable as AlP in ambient air. But an uncapped 25 nm thick $AlP_{013}N_{0.87}$ layer was completely dissolved in the alkaline developer within 60 s during processing attempts. On the positive side, this makes AlPN is an easily removable, lattice matched sacrificial layer.

One uncapped slight compressivly strained 140 nm AlPN layer on GaN/sapphire from the first series (no tBP preflow) was measured by TEM after two months of storage in air and subsequent thinning. As visible in the EDS trace in figure 4 the former $AlP_{0.13}N_{0.87}$ layer contained between 10-20 % oxygen and showed no wurtzite like diffraction patterns (see supplemental). The same sample still showed an AlPN related reflection in XRD half a year later, so the TEM sample oxidized strongly during/after thinning. This is also supported by the energy dispersive X-ray spectroscopy (EDS) trace, since the O signal gets stronger at the thinner upper part of the TEM slice in figure 4 while all other EDS amplitudes decrease. The EDS trace shows also a very abrupt elemental interface between GaN and AlPN, with almost no Ga carry over within the z-resolution of about 5 nm. The right side of figure 4 clearly shows that the Ga/Al transition is as expected, while the Al/P ratio shoots over, i.e. there is a $15 - 30$ nm thick P-deficient AlPN layer directly on the GaN. This P-deficient layer is probably the reason why we sometimes observed also cracking even for lattice matched layers before introducing the tBP preflow.

To conclude, the first layers of tensile strained and lattice matched wurtzite AlP_yN_{1-y} were grown on GaN. Tensile strain respective lattice matching is the key point to avoid phase separation or P antisite defects, because the increase of strain prevents P to occupy an Al site. The P content is mostly controlled by the partial pressure of tBP. A typical growth rate was 650 nm/h at growth conditions close to GaN buffer growth. We found the need for a P pre-flow and P+N stabilisation after AlPN layer growth. The first characterisation results indicate abrupt Ga/Al at the GaN/AlPN interface, i.e. no Ga carry over. Compared to lattice matched AlInN, AlPN has a larger bandgap around 5.5 eV and a higher refractive index contrast, and gives low sheet resistances in high mobility heterostructures.

References

[1] J.-F. Carlin, C. Zellweger, J. Dorsaz, S. Nicolay, G. Christmann, E. Feltin, R. Butté, and N. Grandjean, phys. stat. sol. (b) **242**, 2326 (2005).

[2] M. Hiroki, Y. Oda, N. Watanabe, N. Maeda, H. Yokoyama, K. Kumakura, and H. Yamamoto, J. Crystal Growth **382**, 36 (2013).

[3] R. Bouveyron and M. Charles, J. Crystal Growth **464**, 105 (2017).

[4] K. Zhou, H. Ren, M. Ikeda, J. Liu, Y. Ma, S. Gao, C. Tang, D. Li, L. Zhang, and H. Yang, Superlattices and Microstructures **101**, 323 (2017).

[5] S. Leone, J. Ligl, C. Manz, L. Kirste, T. Fuchs, H. Menner, M. Prescher, J. Wiegert, A. Žukauskaité, R. Quay, and O. Ambacher, phys. stat. solidi (RRL) **14**, 1900535 (2020).

[6] J. Ligl, S. Leone, C. Manz, L. Kirste, P. Doering, T. Fuchs, M. Prescher, and O. Ambacher, J. Appl. Phys. **127**, 195704 (2020).

[7] M. Kume, Y. Ban, K. Harafuji, I. Kidoguchi, S. Kamiyama, A. Tsujimura, R. Miyanaga, A. Ishibashi, and Y. Hasegawa, "Semiconductor laser device," (1999), patent US6466597B1.

[8] K. Iwata, H. Asahi, K. Asami, and S. ichi Gonda, Jap. J. Appl. Phys. **35 Part 2**, L1634 (1996).

[9] R. Kuroiwa, H. Asahi, K. Asami, S.-J. Kim, K. Iwata, and S. Gonda, Appl. Phys. Lett. **73**, 2630 (1998).

[10] T.-Y. Seong, I.-T. Bae, C.-J. Choi, D. Y. Noh, Y. Zhao, and C. W. Tu, J. Appl. Phys. **85**, 3192 (1999).

[11] R. Soni, P. Dobal, R. Katiyar, H. Asahi, H. Tampo, and S. Gonda, MRS Proceedings **618**, 321 (2000).

[12] J. Kikawa, S. Yoshida, and Y. Itoh, J. Crystal Growth **229**, 48 (2001).

[13] S. Yoshida, J. Li, and Y. Itoh, phys. stat. sol. (c) **0**, 2236 (2003).

[14] L. Li-Wu, C. Ting-Jie, S. Bo, W. Jiang-Nong, and G. Wei-Kun, Chin. Phys. Lett. **22**, 2081 (2005).

[15] D. Chen, B. Shen, Z. Bi, K. Zhang, S. Gu, R. Zhang, Y. Shi, Y. Zheng, X. Sun, S. Wan, and Z. Wang, Appl. Phys. A **80**, 141 (2005).

[16] K. Fehse, A. Dadgar, P. Veit, J. Blng, and A. Krost, Appl. Phys. A **82**, 733 (2006).

[17] S. Assali, I. Zardo, S. Plissard, D. Kriegner, M. A. Verheijen, G. Bauer, A. Meijerink, A. Belabbes, F. Bechstedt, J. E. M. Haverkort, and E. P. A. M. Bakkers, Nano Letters **13**, 1559 (2013).

[18] P. Kurpas, J. Jönsson, W. Richter, D. Gutsche, M. Pristovsek, and M. Zorn, J. Crystal Growth **145**, 36 (1994).

[19] X.-L. Wang, A. Wakahara, and A. Sasaki, J. Crystal Growth **129**, 289 (1993).

[20] F. Oehler, M. E. Vickers, M. J. Kappers, and R. A. Oliver, J. Appl. Phys. **114**, 053520 (2013).

[21] K. Persson, "Materials data on AlP (SG:186) by Materials Project," (2014).

[22] A. B. Kuzmenko, Rev. Sci. Instr. **76**, 083108 (2005).

[23] R. Swanepoel, J. Phys. E: Sci. Instr. **16**, 1214 (1983).

[24] Z. Ye, S. Nitta, Y. Honda, M. Pristovsek, and H. Amano, Jpn. J. Appl. Phys. **59**, 025511 (2020).

[25] A. Ishibashi, H. Takeishi, M. Mannoh, Y. Yabuuchi, and Y. Ban, J. Electronic Mat. **25**, 799 (1996).

[26] N. Watanabe, T. Kimoto, and J. Suda, J. Appl. Phys. **104**, 106101 (2008).

[27] R. Tülek, A. Ilgaz, S. Gökden, A. Teke, M. K. Öztürk, M. Kasap, S. Özçelik, E. Arslan, and E. Özbay, J. Appl. Phys. **105**, 013707 (2009).

[28] Y. Terada, Y. Shimogaki, Y. Nakano, and M. Sugiyama, J. Crystal Growth **312**, 1359 (2010).

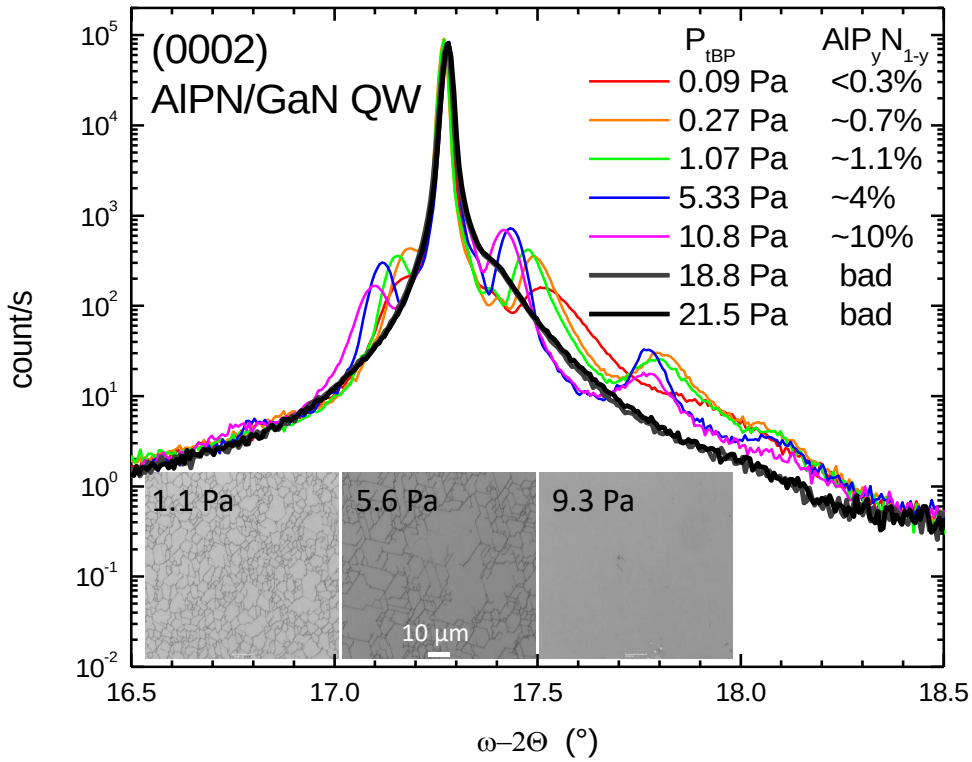

Fig. 1. $\omega - 2\Theta$ measurement of a series of 5× AlPN/GaN quantum wells around the (0002) GaN reflection. Thicker lines indicate nominally compressively strained layers. Inset shows three Nomarski microscopy images of 20-45 nm thick AlPN films grown on GaN. Partial pressures were TMAl 0.23 Pa, and NH_3 20.5 Pa at 1100˚C.

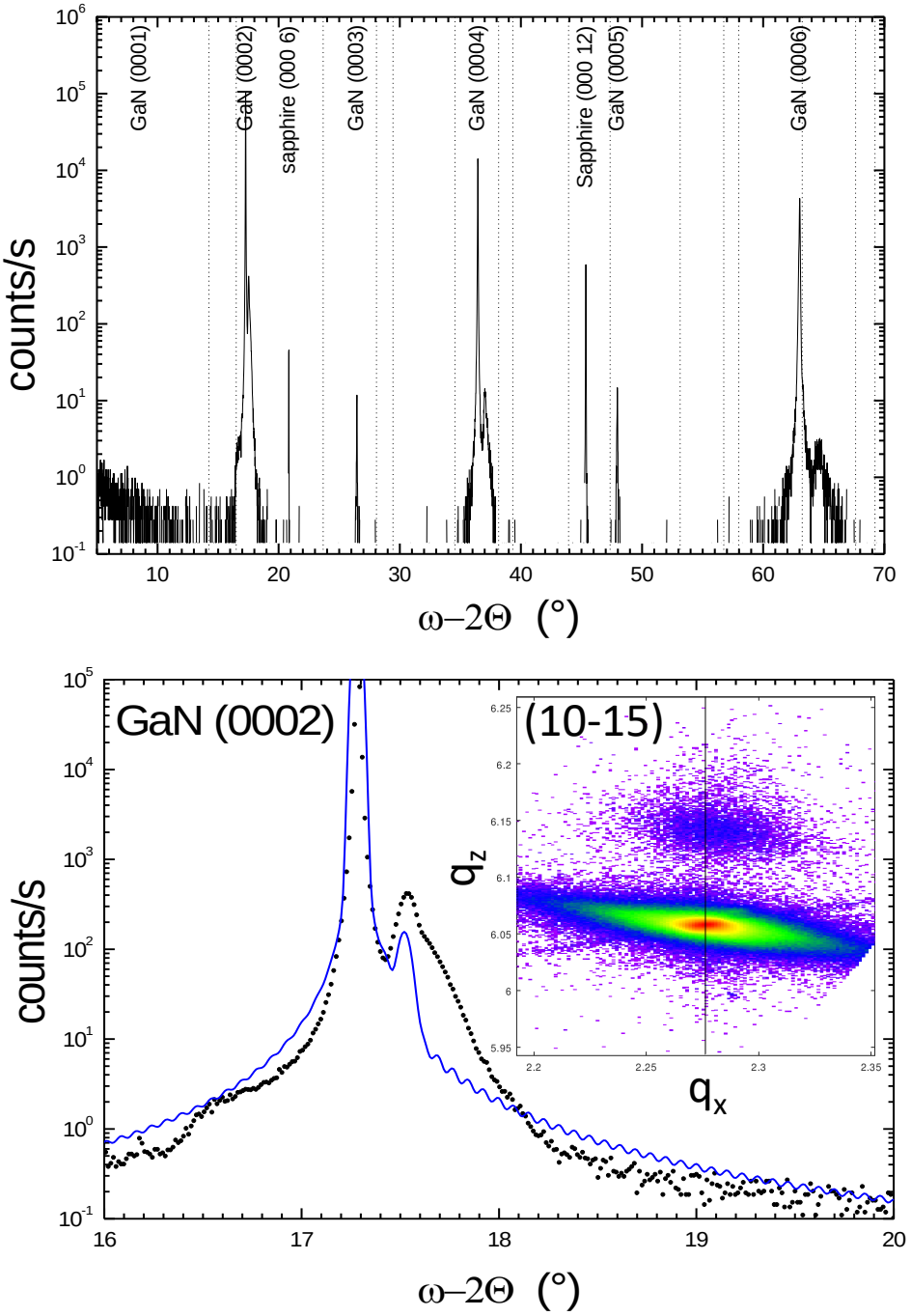

Fig. 2. Wide area $\omega - 2\Theta$ measurement of a nearly lattice matched 60 nm AlPN layer on GaN (top). The dotted lines indicate all allowed cubic AlP reflections. Bottom is a high resolution $\omega - 2\Theta$ measurement around (0002) of the same sample with simulation of a 60 nm $AlP_{10.3}N_{89.7}$ layer. The inset is the $(10\bar{1}5)$ reciprocal space map showing a perfectly strained AlPN layer.

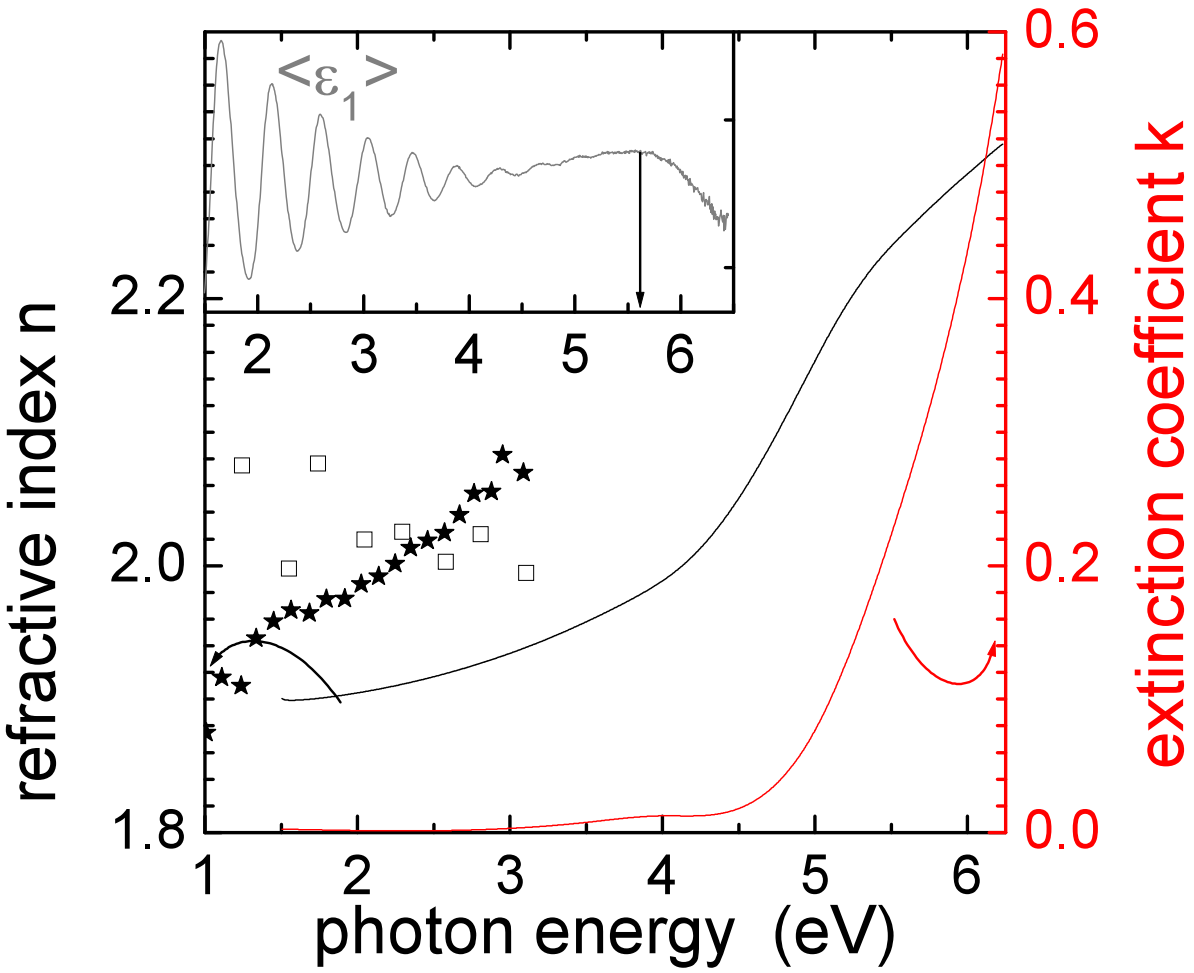

Fig. 3. Refractive index and extinction coefficient averaged from three $AlP_{0.13}N_{0.87}$ layers of 180 nm, 315 nm and 655 nm on GaN-sapphire. The points are from vertical incidence reflection measurements of a 315 nm (open box) and 655 nm (star) AlPN layer. The inset shows the effective $< \epsilon_1 >$ data of a 655 nm $AlP_{0.13}N_{0.87}$layer on 22 μm carbon doped GaN on sapphire, to suppress GaN FP oscillations.

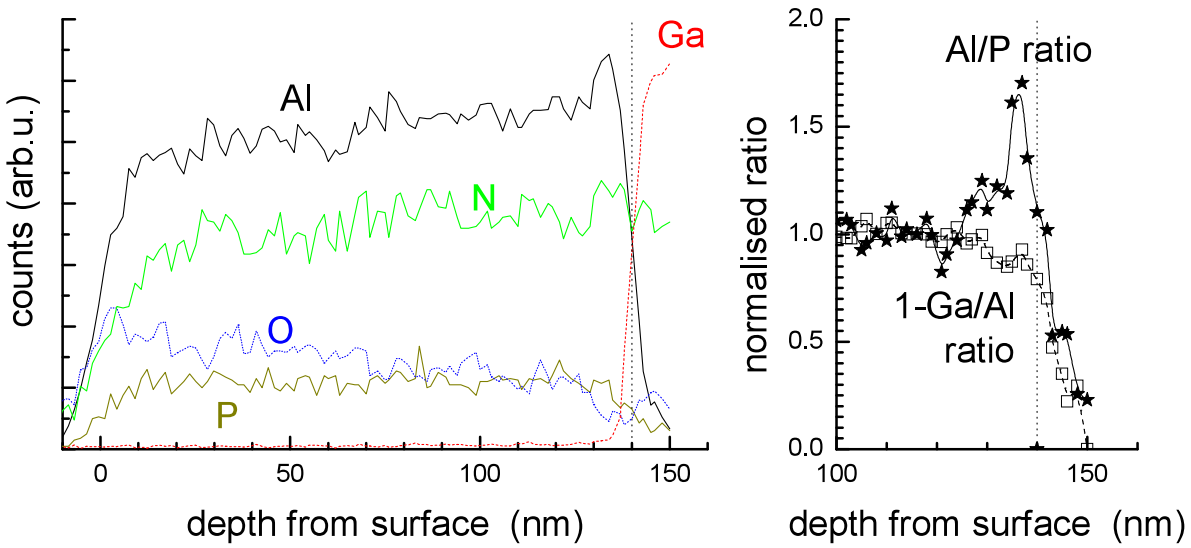

Fig. 4. TEM-EDS trace from a 140 nm AlPN layer after storage in air for about 2 months (left). The Ga signal is reduced by $\frac{2}{3}$ while N, P, and O signals are multiplied by 2.5. The gradient of the EDS signal amplitudes towards the surface originates from the wedge shape of the TEM slice. The vertical line marks the interface to GaN according to TEM. Right side shows the normalised (1-Ga)/Al ratio (open box) and the Al/P ratio (star).